CORROSION SCIENCE AND TECHNOLOGY, Vol.10, No.2(2011), pp.60~64

Corrosion Properties of Duplex Stainless Steels - STS329LD and STS329J3L - for the Seawater Systems in Nuclear Power Plant

Hyun-Young Chang, Heung-Bae Park, Young-Sik Kim[1], Sang-Kon Ahn[2], and Yoon-Young Jang[3,†]

Korea Electric Power Corporation E&C, Yongin, Republic of Korea
[1]Materials Research Center for Energy and Green Materials Technology, School of Advanced Materials Engineering, Andong National University, 388 Songcheon, Andong, Gyeongbuk 760-749, Korea
[2]POSCO, Pohang, Republic of Korea, [3]ANSCO, Daejeon, Republic of Korea
(Received January 28, 2011; Revised March 10, 2011; Accepted March 11, 2011)

Lean duplex stainless steels have been developed in Korea for the purpose of being used in the seawater systems of industry. There are also many important seawater systems in nuclear power plants. These systems supply seawater to cooling water condenser tubes, heat exchanger tubes, related pipes and chlorine injection systems. The flow velocity of some part of seawater systems in nuclear power plants is high and damages of components from corrosion are severe. The considered lean duplex stainless steels are STS329LD (20.3Cr-2.2Ni-1.4Mo) and STS329J3L (22.4Cr-5.7Ni-3Mo) and PRENs of them are 29.4 and 37.3 respectively. Physical, mechanical and micro-structural properties of them are evaluated, and electrochemical corrosion resistance is measured quantitatively in NaCl solution. Critical Pitting Temperatures (CPT)s are measured on these alloys and pit depths are evaluated using laser microscope.
Long period field tests on these alloys are now being performed, and some results are going to be presented in the following study.

Keywords *: duplex stainless steel, nuclear power plant, critical pitting temperature*

1. Introduction

Stainless steels are composed of various alloying elements. In duplex stainless steels, particularly, a combination of alloying elements is very important because of the ratio of ferrite and austenite phases. Duplex stainless steels can be categorized on the base of $PREN_{30}$ as follows;[1)-7)] the alloys under 40 of $PREN_{30}$ are composed of Cr: 21~23%, Mo: 1~3%, Ni: 5~7% N: 0.1~0.25%, and the alloys in the range of 40~50 of $PREN_{30}$ possess Cr: 24~26%, Mo: 2~4%, Ni: 6~7% N: 0.2~0.3%, and the alloys over 50 of $PREN_{30}$ have Cr 25~28%, Mo: 4~6%, Ni: 6~9%, W: 1~5% N: 0.3~0.4%. In order to make a higher $PREN_{30}$ of alloy in general, chromium content should be increased. In addition, Mo, W, and N were added to improve the localized corrosion resistance and mechanical properties. Furthermore, Ni content was increased to control the ratio of α/γ and enhance the corrosion resistance.

† Corresponding author: hyjang@kepco-enc.com

Ni in the passive film exists as Ni^{2+} and NiO,[8)] and NiO and hydrated NiO.[9)-11)] Also, Ni reduces the critical passive current density (i_c) in the polarization curve and then facilitates the passivation.[12)] That is, the passive current density (i_p) and primary passive potential (E_{pp}) are lowered and pitting potential (E_p) increases. With increasing Ni content, the ratio of ferrite phase is reduced. Fe-xCr-yNi alloys are sensitive to SCC in the range of 8~12% Ni but its resistance increases below or above its range.[13),14)] Common duplex stainless steels have 5~9% Ni, which increases pitting resistance, cavitation resistance, and bending fatigue strength of them. On the other hand, Fe-xCr-yNi-3Mo-0.15N alloys shows lowered corrosion resistance when Ni content is reduced below 4% and thus it is suggested that Cr content should be over 22% when the alloys have below 4% Ni.[3),15)]

Ni plays important role in stainless steels as reviewed above, but low Ni duplex stainless steels have been still developed because of the expensive Ni cost.

In this work, lean duplex stainless steels of STS329LD

.3Cr-2.2Ni-1.4Mo-0.15N) and STS329J3L (22.4Cr-Ni-3Mo-0.16N) were manufactured. Mechanical and :ro-structural properties of them are evaluated, and elec-:hemical corrosion resistance is measured quantitatively NaCl solution. Chemical corrosion resistance is also luated.

Experimental

The stainless steels evaluated in this study were pre-ed from commercially produced ingot and hot-rolled tes by POSCO. The hot rolled specimens were annealed 1,025 ℃ for 10 minutes, water quenched, and acid kled. A small section was cut after each procedure and s used for chemical analysis.

Specimens for optical microscopic analysis were pre-ed from cutting the plate to pieces in size 1.5 x 1.5 . They were fixed in epoxy resin and polished using SiC paper up to #2000. Vibration polisher was used for :cimen to have mirror surface. The composition of elec-lytic etching solution for microscopic analysis was 30 % KOH (2V, 10sec). Specimens for hardness tests were pared by the same procedures as those of optical micro-pic analysis and micro-Vickers hardness of them were asured.

The experimental alloys were subjected to anodic polar-tion in 0.1%, 1.0%, 3.5% NaCl solution at 30 ℃. A entiostat (Gamry DC 105) was used in the anodic polar-tion test. The specimen was polished to #600 using Sic per. After rinsing them, their surfaces were covered by oxy resin with only 1 cm^2 of surface area being exposed test solution. The solution was deaerated by purging m with pre-purified nitrogen gas for 30 minutes at a e of 100 ml/min. prior to immersion of the specimen. ter immersion, a cathodic potential of -200 mV(SCE) low its corrosion potential was applied to the specimen 10 min. The specimen was then maintained for 10 n. at an open circuit potential, and subsequently polar-d anodically from its corrosion potential at a scanning e of 1 mV/min. A saturated calomel electrode (SCE) s used as a reference electrode and high-density graphite ds as counter electrodes.

The critical pitting temperature was measured by the thod described in ASTM G48-03.[16] Test solution was 6% $FeCl_3$ + 1% HCl and the specimen was polished to #120 using a SiC paper. The starting temperature was based on ASTM G48-03 and the specimen was immersed for 24 hours at each temperature.

3. Results and discussion

Table 1 shows the chemical compositions of duplex stainless steels produced by POSCO. STS329LD has Fe-20.3Cr-2.2Ni-1.4Mo-0.15N and STS329J3L consists of Fe-22.4Cr-5.7Ni-3.1Mo-0.16N. Fig. 1 shows the optical microstructures of duplex stainless steels; (a) STS329LD and (b) STS329J3L. White portions are austenite phase and dark portions are ferrite phase. Ferrite phase is longitudinally stretched by rolling work.

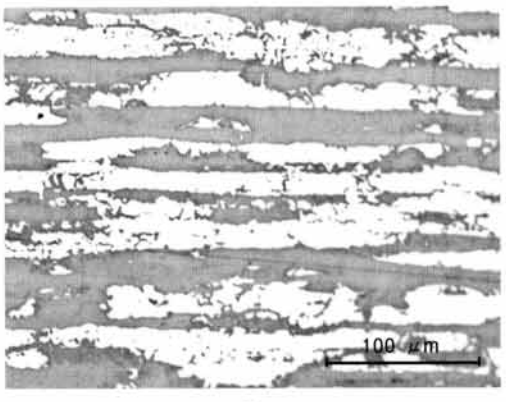

(a)

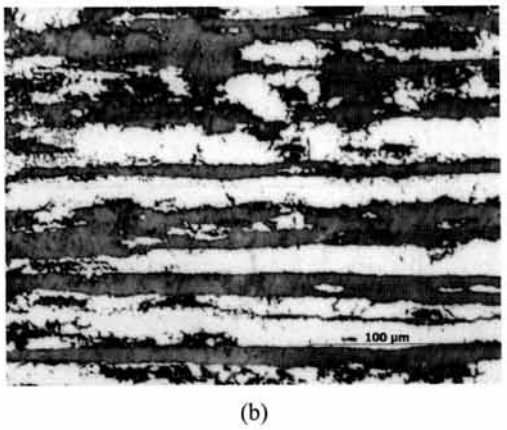

(b)

Fig. 1. Optical microstructures of duplex stainless steels; (a) STS329LD, (b) STS329J3L.

able 1. Chemical compositions of duplex stainless steels made by POSCO (unit: wt%)

	C	Si	Mn	P	S	Ni	Cr	Mo	Cu	N	Fe	PREN
STS329LD	0.02	0.58	2.45	0.021	0.0004	2.2	20.3	1.4	0.02	0.15	Bal.	29.4
STS329J3L	0.03	0.58	1.16	0.026	0.0009	5.7	22.4	3.1	0.1	0.16	Bal.	37.3

Ferrite content was measured by the image analyzer. Fig. 2 shows the ferrite contents of the experimental alloys. Ferrite content of STS329LD was 50.9% and its content of STS329J3L was 57.6%.

Fig. 3 shows the micro-Vickers hardness on austenite and ferrite phases of duplex stainless steels. Regardless of phases, the hardness of STS329J3L was higher than that of STS329LD. Regardless of the alloys, the hardness of the ferrite phase was also higher than that of the austenite phase. However, the hardness of austenite in STS329J3L was higher than that in STS329LD in comparison with those of ferrite phases. It seems to be attributed to the ferrite content of the alloys. In other words, since austenite content in STS329J3L is lower than that in STS329LD and nitrogen contents in two alloys are similar, nitrogen concentration of the austenite in STS329J3L may be higher than that in STS329LD and thus the hardness of austenite in STS329J3L was higher than that in STS329LD.

Fig. 4 shows polarization curves of (a) STS329LD and (b) STS329J3L in deaerated 30 ℃, 0.1% NaCl, 1% NaCl, 3.5% NaCl solutions. In case of STS329LD, the pitting potential decreases as chloride concentration increases. However, pitting potential is similar to the oxygen evolution potential in case of STS329J3L.

Fig. 5 shows a process for determining Critical Pitting Temperature (CPT) according to ASTM G48 Method E; (a) for STS329LD and (b) for STS329J3L. The red horizontal dotted lines in these figures mean the pit-indicative criterion - 0.1 mg/cm^2. In case of 329LD, the weight loss at 20 ℃ is under the pit-indicative criterion but weight

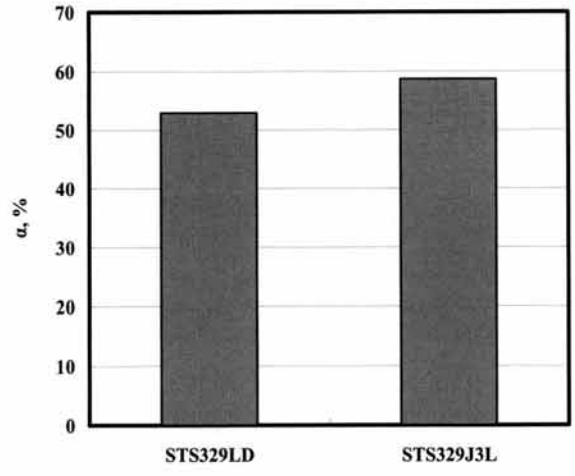

Fig. 2. Ferrite contents of duplex stainless steels.

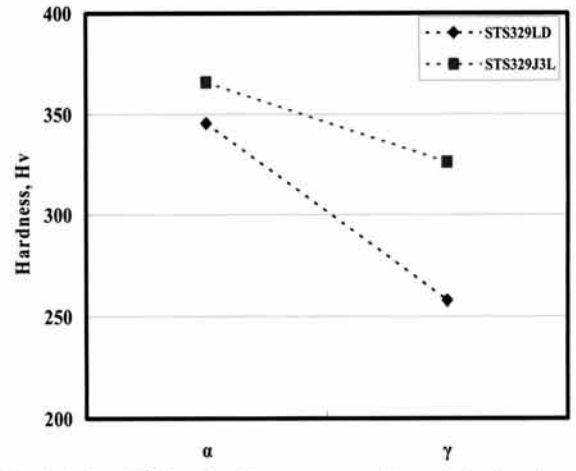

Fig. 3. Micro-Vickers hardness on austenite and ferrite phases of duplex stainless steels.

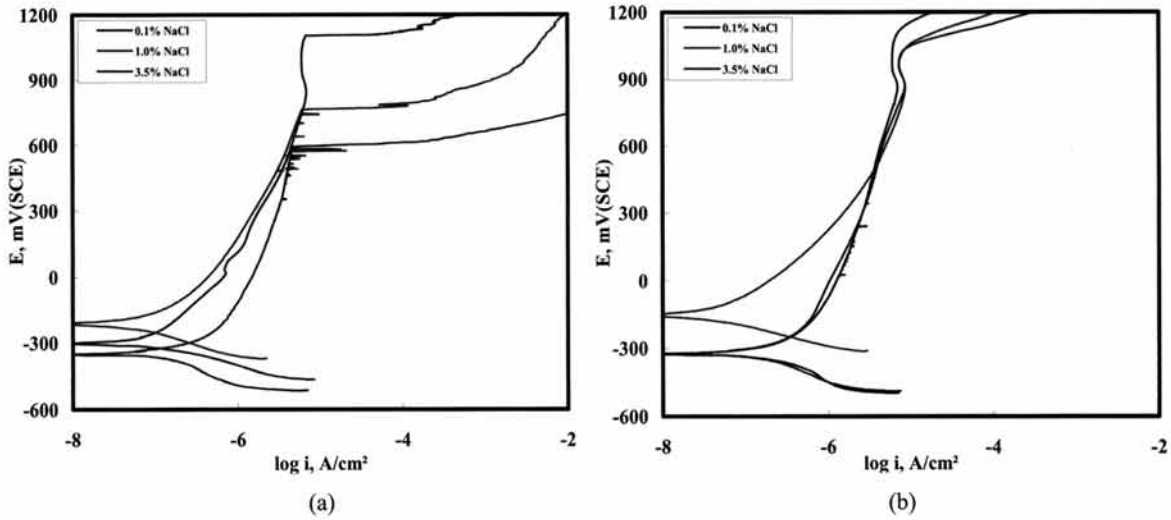

Fig. 4. Polarization curves of (a) STS329LD and (b) STS329J3L in deaerated 30 ℃, 0.1% NaCl, 1% NaCl, 3.5% NaCl solutions.

losses at 25, 30 ℃ exceed the pit-indicative criterion. 329J3L shows weight losses under the pit-indicative criterion at 30, 35, 40 ℃ but weight loss at 45 ℃ exceeds the pit-indicative criterion. ASTM G48 recommends a visual examination for measurement of pitting initiation such as photographic reproduction when mass loss corrosion rate is greater than or equal to 0.1 mg/cm^2. The specification also specifies that a more detailed examination will include the measurement of maximum pit depth, average pit depth, pit density using needle point micrometer gauge

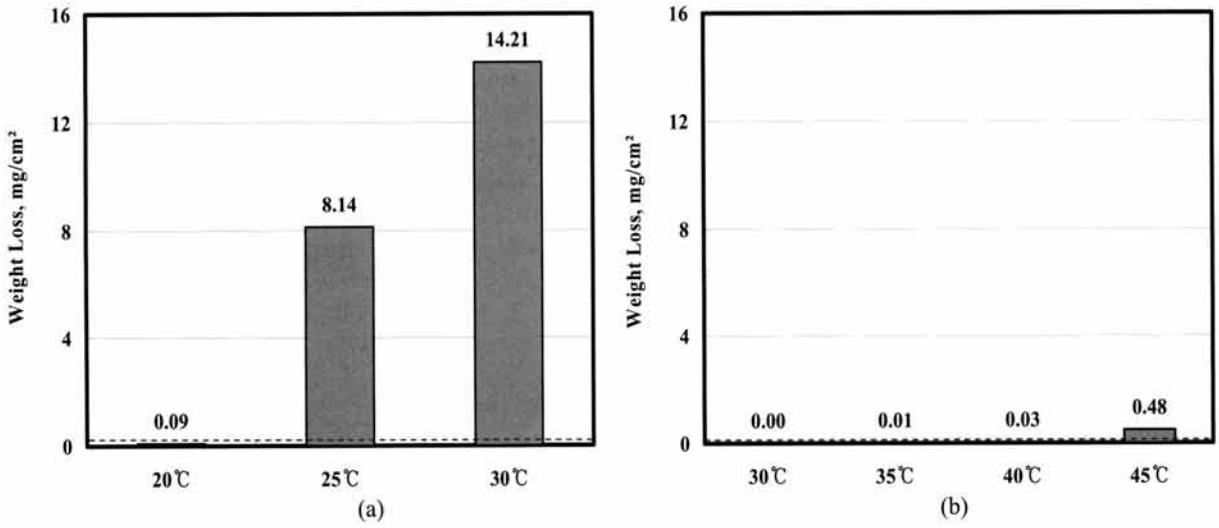

Fig. 5. A process for determining CPT according to ASTM G48 Method E; (a) STS329LD, (b) STS329J3L (horizontal dotted line means the pit-indicative criterion - 0.1 mg/cm^2.

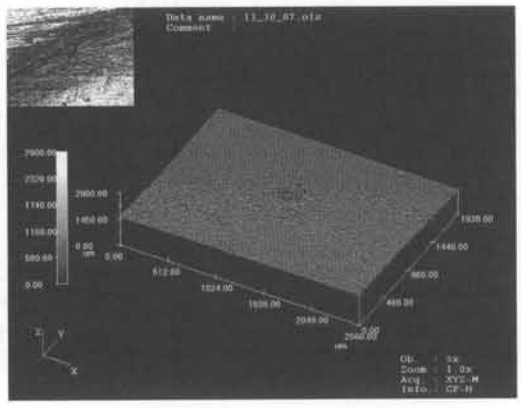

(a)

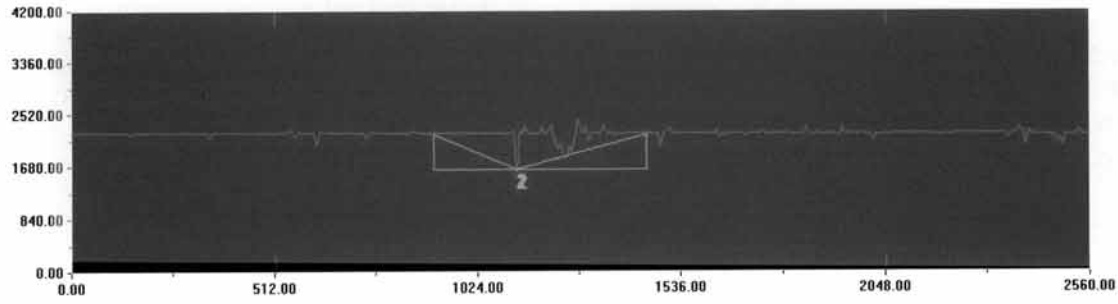

(b)

Fig. 6. (a) 3D image and (b) depth profile for determining a pitting using a confocal laser scanning microscope of STS329J3L after 24hours-immersion in 45 ℃, 6% $FeCl_3$ + 1% HCl solution.

Table 2. Test result of pitting corrosion of STS329J3L by ASTM G48-03 method E

Test temperature	30℃	35℃	40℃	45℃
Weight loss(mg)	0	0.1	0.2	3.6
Weight loss(mg/cm^2)	0	0.01	0.03	0.48
Pit or not by ASTM G48(>0.1mg/cm^2)	none	none	none	yes
Pit or not by penetration test	none	none	none	yes
Pit or not by ASTM G48 (>25μm)	none	none	none	556.4μm
CPT				45℃

or microscope with calibrated fine-focus knob or calibrated eyepiece. In this work, another method was applied; the penetration test to find pit sites and pit depth measurement using a confocal laser scanning microscope (Olympus, LEXT OLS-3000). Fig. 6(a) shows 3D image on pitted surface and Fig. 6(b) is a depth profile for determining a pit using a confocal laser scanning microscope of STS329J3L after 24 hour-immersion in 45 ℃, 6% $FeCl_3$ + 1% HCl solution. The penetration test and confocal laser scanning microscope could measure locations of pits and the exact pit depths. Table 2 is the summary of CPT determining process of STS329J3L. In case of 45 ℃ test, weight loss of the alloy exceeds the pit-indicative criterion and pit site is detected by the penetration test. The pit depth of it was measured as 556.4 μm by the confocal laser scanning microscope. Finally, CPT of STS329J3L was determined as 45 ℃.

4. Conclusions

1) The chemical compositions of duplex stainless steels by POSCO were Fe-20.3Cr-2.2Ni-1.4Mo-0.15N (STS329LD) and Fe-22.4Cr-5.7Ni-3.1Mo-0.16N (STS329J3L). Ferrite phase was longitudinally stretched by rolling works and its contents of STS329LD and STS329J3L were 50.9% and 57.6% respectively.

2) The hardness of austenite of STS329J3L is higher than that of STS329LD in comparison of those of the ferrite phase. It seems to be due to the ferrite content of the alloys. In other words, since austenite content inSTS329J3L is lower than that in STS329LD and nitrogen contents in two alloys are similar, nitrogen concentration of the austenite in STS329J3L may be higher than that in STS329LD.

3) The penetration test and the confocal laser scanning microscope made it possible to measure the location of pits and the exact pit depths. CPT determining process includes weight loss measurement, pit site identification by the penetration test and pit depth measurement by the confocal laser scanning microscope. Finally, CPTs of STS329LD and STS329J3L were determined as 25 ℃ and 45 ℃ respectively.

References

1. A. J. Sedriks, *Corrosion of Stainless Steels*, John Wiley & Sons, Inc., (1996).
2. H. S. Park and Y. S. Park, *J. Corros. Sci. Soc. of Kor.*, **28**, 59 (1999).
3. J. S. Kim, C. J. Park, and H. S. Kwon, *Bul. Kor. Inst. Met. & Mater.*, **12**, 635 (1999).
4. M. Snis and J. Olsson, *Desalination*, **223**, 476 (2008).
5. J. H. Shin and J. B. Lee, *J. Kor. Int. Surf. Eng.*, **39**, 18 (2006).
6. H. S. Park and Y. S. Park, *J. Corros. Sci. Soc. of Kor*, **28**, 78 (1999).
7. H. S. Park and Y. S. Park, *J. Corros. Sci. Soc. of Kor*, **28**, 108 (1999).
8. S. M. Wilhelm and N. Hackerman, *J. Electrochem. Soc.*, **128**, 1668 (1981).
9. C. Sunseri, S. Piazza, and F. D. Quarto, *Mater. Sci. Forum*, **185**, 435 (1995).
10. P. Marcus, J. Oudar, and I. Olefjord, *J. Microsc. Spectrosc. Electron*, **4**, 63 (1979).
11. S. Fujimoto, H. Tsuchiya, M. Sakamoto, T. Shibata, and K. Asami, 201st *Meeting of the Electrochemical Society*, 278 (2002).
12. Y. T. Jeon, U. H. Joo, Y. S. Kim, and Y. S. Park, *J. Corros Sci. Soc. of Kor*, **29**, 133 (2000).
13. A. J. Sedriks, *Corrosion*, **42**, 376 (1986).
14. H. R. Copson, *Physical Metallurgy of SCC Fracture*, p. 247 Interscience, New York (1959)
15. K. Osozawa and H. J. Engell, *Corros. Sci.*, **6**, 389 (1966).
16. ASTM G48-03, Standard Test methods for Pitting and Crevice Corrosion Resistance of Stainless Steels and Related Alloys by Use of Ferric Chloride Solution.